DOI: 10.1021/ma902576q

Macromolecules
ARTICLE

Modeling and Understanding Smectic-Phase Formation in Binary Mixtures of Rodlike Polysilanes: Comparison of Onsager Theory and Experiment

Szabolcs Varga*,†

Departamento de Física Teórica de la Materia Condensada, Universidad Autónoma de Madrid, E-28049 Madrid, Spain. †Permanent address: Institute of Physics, University of Pannonia, PO Box 158, Veszprém, H-8201 Hungary.

Enrique Velasco

Departamento de Física Teórica de la Materia Condensada and Instituto de Ciencia de Materiales Nicolás Cabrera, Universidad Autónoma de Madrid, E-28049 Madrid, Spain

Received November 23, 2009; Revised Manuscript Received March 17, 2010

ABSTRACT: We study a binary mixture of short and long parallel hard rods in the smectic A phase to understand the role of length ratio (weight ratio) in the formation of three different types of ordering which were observed in binary mixtures of helical polysilanes. Using Onsager's second virial theory of parallel hard rods, and modeling the short and long polymers as hard cylinders of different lengths ($L_1 \neq L_2$) and same diameters (D), we show that the normal smectic A phase (S_1) forms for length ratios ($l = L_2/L_1$) between 0.58 and 1, the microsegregated smectic structure (S_2) takes place for $0.32 < l < 0.56$ and $0 < l < 0.39$ in short-rod-rich and long-rod-rich phases, respectively, and the two-in-one ordering (S_3) is stable only in mixtures rich in long rods for $0.33 < l < 0.58$. These results are in very good agreement with the available experimental data of binary mixtures of polysilanes [Okoshi et al. *Macromolecules* **2009**, *42*, 3443]. In addition, the theory predicts the existence of a partially microsegregated smectic structure (S_4), in long-rod-rich mixtures, for $0.3 < l < 0.39$. Our theoretical results show that two or even three smectic order parameters should be measured, for *all* types of smectic phases, in order to obtain the correct positional distribution functions from the X-ray diffraction pattern.

1. Introduction

It is now generally accepted that hard-body interactions play a crucial role in the structural properties and phase transitions of simple and complex fluids.[1] Even the formation of mesophases (nematic, smectic, columnar, etc.) is mainly due to the excluded volume interaction through short-range anisotropic repulsions between rodlike or platelike molecules (e.g., see refs 2−4). In the seminal paper of Onsager,[5] it was proved that even a second virial theory is capable of describing accurately the isotropic−nematic phase transition of long and thin hard rods. After Onsager, a considerable number of theoretical, simulation, and experimental studies were performed to clarify the role of excluded-volume interactions in the stability of mesophases.[6] While it is not difficult to study hard-body fluids by Onsager-type theory and Monte Carlo simulation, it is still a big challenge for experimentalists to create a model system in which molecules interact only through hard-body repulsions. Well-known experimental examples are sterically- or charged-stabilized colloidal liquid crystals made of mineral particles (goethite, boehmite, etc.),[7] or aqueous solutions of biological macromolecules (proteins, DNA)[8] and viruses (TMV, fd).[9] The phase behavior of these systems is more or less mimicked by hard-body fluids, but polydispersity, flexibility, surface charges, and chiral interactions may have a very strong influence on the phase-transition properties. For example, large polydispersities in both particle length and diameter considerably increase the width of the isotropic−nematic biphasic region of boehmite nanorods as compared with that of the corresponding monodisperse hard rods.[10] Also, the smectic phase is known not be stable in colloidal-rod fluids with length polydispersity in excess of 18%.[11,12] For these reasons, the agreement between the phase behavior of monodisperse hard-body fluids and the experimental systems is only qualitative.

Recently, a very promising thermotropic liquid crystal has been synthesized to study the role of excluded-volume interactions in the stability of mesophases.[13] Watanabe et al. showed that a nearly monodisperse system of polysilanes forms isotropic, nematic/cholesteric, smectic, and columnar phases upon decreasing the temperature, the constituting polymer particles being very rigid, rodlike, and nonpolar. In one type of polysilanes (PD2MPS),[13b] the polymers are not chiral and the normal nematic phase takes place, while in the other type of polysilanes (PD2MBS),[13a] chirality induces a twisted nematic structure. Interestingly, the structure of the smectic phase is not affected by chirality, which means that the chiral strength is weak even in the PD2MBS polymer. From the theoretical point of view, the only drawback of these systems is that phase transitions are not only density-dependent, as in the case of hard-body fluids, but also temperature-dependent. Therefore, a proper theoretical description of polysilanes requires the inclusion of dispersion interactions into the model potential. In spite of this, the hard-body pair potential can be a good approximation at high temperature.

Experimental attempts to create binary mixtures of hard-body liquid crystals are quite rare. van der Kooij and Lekkerkerker studied a very polydisperse binary mixture of rods and plates.[14] The fd-viral particles were used by Purdy et al.[15] to investigate the

*To whom correspondence should be addressed.

 Published on Web 03/31/2010

phase behavior of binary mixtures of thin (fd-) and thick (PEG-coated fd-) viruses of the same length. However, both of these systems are still far from the ideal hard-body mixture. By contrast, there are several theoretical works in the literature devoted to binary mixtures of short and long hard rods[16−22] and those of thin and thick rods.[23−25] Most of these studies focus on the determination of the global phase diagram, which includes ordering transitions (isotropic−nematic, nematic−smectic, etc.), fractionation effects, and nematic−nematic and smectic−smectic demixing transitions. The main conclusion of these studies is that the accommodation problem between the short and long rods induces columnar ordering, while destabilizing the smectic phase with respect to the nematic and columnar phases. These findings are also confirmed by MC simulation studies.[19] Interestingly, only a few studies[16−18,20,21] deal with the structure of the surviving smectic A phase, in which the efficient packing of short and long rods is not a trivial issue, even though Koda and Kimura,[16] in their early work, already reported about possible microsegregation effects taking place between the two components in smectic phases rich in both short and long rods. To determine the effect of orientational freedom on the stability of isotropic, nematic and smectic phases, Cinacchi et al.[17,20] have examined the binary mixture of freely rotating hard rods using a rescaled Onsager theory. The main result from studies of freely rotating rods[17,20,21,25] is that the orientational entropy favors segregation and widens the biphasic region of the nematic−smectic phase transition.

After a long latency period, a renewed interest has arisen from the very recent work of Okoshi et al.,[26] who have examined the smectic A phase properties of a binary mixture of short and long polysilanes at high temperature (T = 100 °C). Depending on the weight ratio (length ratio), three types of smectic A structures are detected: the conventional smectic A phase; the microsegregated smectic phase; and a third type of ordering, the so-called *two-in-one* layering, where two layers of short rods accommodate into one layer of long rods. Because of the relatively high temperature and the narrow molecular weight distributions of both species, the binary mixture of PD2MBS polymers can be considered as an appropriate playground for testing the reliability of hard-body theories. The occurrence of the new, two-in-one smectic structure was first confirmed in our previous theoretical work,[18] where the global phase diagram of the mixture was determined using Onsager theory for parallel rods. However, no simulation studies have been undertaken for two-in-one smectic ordering yet. In the present paper we focus on the determination of the molecular requirements necessary for the stability of two-in-one ordering, and compare our results with the available experimental data,[26] by modeling the binary mixture of polysilanes as a mixture of short and long parallel hard cylinders. As a first step, we do not include orientational entropy effects, which complicate the numerical calculation significantly. We discuss the repercussions of this approximation in the concluding section.

The outline of the paper is as follows. In section 2, the molecular model for a binary mixture of polymers and a brief overview of Onsager theory for the smectic A phase are presented. Detailed comparison between the theory and experiment is made in section 3. Finally, we make some concluding remarks in section 4.

2. Model and Theory

The dominant interaction between the polymers in the smectic phase of PD2MBS is hard-repulsive because of charge neutrality and shape rigidity. Since polysilanes are thermotropic liquid crystals, dispersive interactions also have some influence on the phase behavior of the system, especially at low temperatures. However, attractive interactions may be completely ignored in the model at high temperatures. To make the theoretical model of polysilanes as simple as possible, it is reasonable to assume, as a first approximation, that a polysilane polymer molecule can be considered as a rodlike hard body. We use the hard-cylinder model with characteristic length (L) and diameter (D). As we study a binary mixture of short and long polymers, both components have equal diameters, while their lengths are different and labeled as L_1 and L_2. The effects of anisotropic attractions and molecular weight polydispersity are ignored in the model. The simplest possible theoretical framework to investigate a fluid of hard cylinders is the Onsager theory. This theory has been used to analyze the phase behavior of several one-component fluids,[27,28] including dimerizing cylinders[29] where the relative stability of smectic and columnar phases was studied. Also, it has been applied to fluid mixtures. For example, the stability of nematic, smectic, and columnar ordering was considered in mixtures of hard rods by Sear and Jackson.[30] Koda and Kimura[16] studied possible smectic structures using the parallel-particle approximation and instability analyses, and Cinacchi et al.[20] relaxed this restriction and performed minimizations with conventional smectic trial functions, obtaining demixing transitions between two different smectic phases.

Restricting ourselves to the smectic phase, we assume that the spatial ordering takes place along the z-axis of the Cartesian coordinate system, while there is no positional order in the $x-y$ plane. Using Onsager's second-virial theory for parallel rods,[16] i.e., with the long axes of the cylinders oriented along the z-axis (parallel-particle approximation), the ideal (F_{id}) and the residual (F_{res}) free energy contributions to the total free energy ($F = F_{id} + F_{res}$) are given by[18]

$$\frac{\beta F_{id}}{V} = \frac{1}{d}\sum_{i=1}^{2}\int_0^d \mathrm{d}z\ \rho_i(z)[\ln\ \rho_i(z) - 1] \tag{1}$$

$$\frac{\beta F_{res}}{V} = \frac{1}{2d}\pi D^2 \sum_{i,j=1}^{2}\int_0^d \mathrm{d}z_1\ \rho_i(z_1) \int \mathrm{d}z_2\ \rho_j(z_2)\Theta\left(\frac{L_i + L_j}{2} - |z_{12}|\right) \tag{2}$$

where $\beta = 1/k_B T$, V is the volume of the reservoir, d is the smectic period, $\rho_i(z)$ is the local number density of the ith component (i = 1, 2), $\Theta(z)$ is the Heaviside step function, and $z_{12} = z_1 - z_2$. In eq 2, the Θ function is derived from the Mayer function of two parallel cylinders and defines the overlap region between cylinders with diameters D and lengths L_i and L_j. Detailed derivation of the free energy terms is presented in our previous work.[18] We must also mention that the ideal free energy term is exact, while the residual one is approximate due to the neglect of the contribution from higher virial coefficients. The equilibrium smectic structure of the binary mixture is determined by those density profiles which minimize the free energy of the system.

In line with earlier analyses of X-ray diffraction patterns of the smectic phase,[31−34] we introduce the positional distribution function of the molecular centers and use the Fourier parametrization method to determine the experimentally measurable smectic order parameters. The positional distribution functions are given by the ratio of local and mean number densities, i.e., $f_i(z) = \rho_i(z)/\rho_i (i = 1, 2)$, where $\rho_i = N_i/V$ and N_i is the number of particles of component i. The Fourier representation of $f_i(z)$ is just a sum of cosine functions weighted by the corresponding Fourier coefficients (f_{ij}), i.e.

$$f_i(z) = \sum_{j=0}^{n} f_{ij}\cos(jqz) \tag{3}$$

where $q = 2\pi/d$ is the smectic wavenumber. It is worthwhile mentioning here that the f_{ij} coefficients are related to the well-known smectic order parameters (τ_{ij}) through $\tau_{ij} = f_{ij}/2$. Note that the

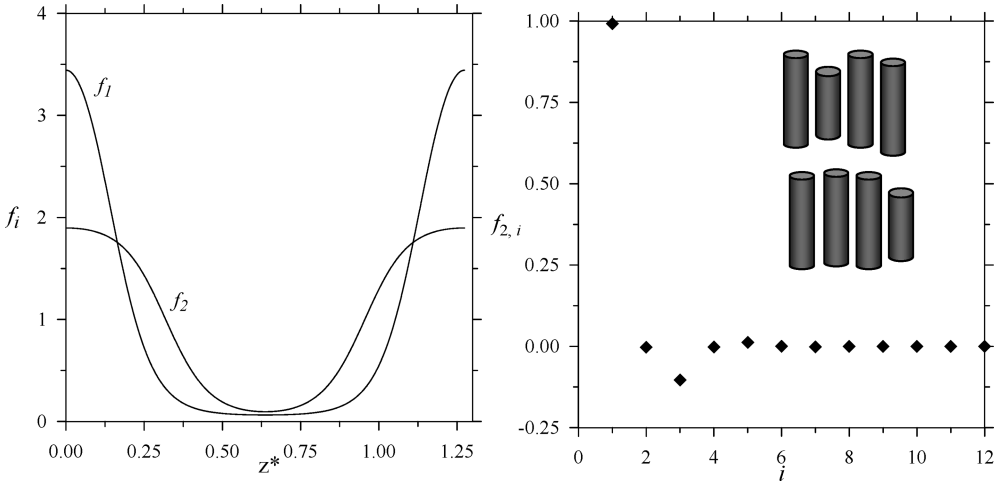

Figure 1. Conventional smectic phase (S_1) at $P^* = 4$ and for $l = 0.65$ and $x = 0.75$. Left panel: positional distribution functions of short and long rods as a function of $z^* = z/L_1$ in the interval $0 < z^* < d/L_1$. Right panel: Fourier spectrum of the short rods and the schematic of particle arrangement in S_1 structure.

zeroth-order Fourier coefficients (f_{10}, f_{20}) are equal to unity since $\rho_i = (1/d)\int_0^d \mathrm{d}z\, \rho_i(z)$. Substitution of eq 3 into eq 2 makes possible to perform the integrations analytically. The resulting residual free energy density is given by

$$\frac{\beta F_{\mathrm{res}}}{V} = \frac{1}{2}\sum_{i,j=1}^{2} \rho_i \rho_j V_{\mathrm{exc}}^{ij} + \frac{1}{2}\pi D^2 \sum_{i,j=1}^{2} \rho_i \rho_j \sum_{k=1}^{n} f_{ik} f_{jk} \sin\left(kq\left(\frac{L_i + L_j}{2}\right)\right)/kq \qquad (4)$$

where $V_{\mathrm{exc}}^{ij} = \pi D^2 (L_i + L_j)$ is the excluded volume between a particle of component i and another particle of component j. The ideal free energy density can also be written down in terms of Fourier coefficients, but it is nonanalytical:

$$\frac{\beta F_{\mathrm{id}}}{V} = \sum_{i=1}^{2} \rho_i (\ln\ \rho_i - 1) + \frac{1}{d}\sum_{i=1}^{2} \rho_i \sum_{j=0}^{n} f_{ij} \int_0^d \mathrm{d}z \cos(jqz) \ln \sum_{k=0}^{n} f_{ik} \cos(kqz) \qquad (5)$$

The evaluation of the integrals in eq 5 is performed using the well-known Simpson formula. We can see from eqs 4 and 5 that the free energy depends on the Fourier coefficients of the two components ($f_{11}, ..., f_{1n}, f_{21}, ..., f_{2n}$) and on the wavenumber (q). To determine them at given density and composition for particular values of molecular parameters, we minimize the total free energy density, which is given by the sum of eqs 4 and 5, as follows:

$$\frac{\partial\left(\frac{\beta F}{V}\right)}{\partial f_{1,j}} = 0, \quad \frac{\partial\left(\frac{\beta F}{V}\right)}{\partial f_{2,j}} = 0 \qquad (j = 1, ..., n) \qquad (6)$$

and

$$\frac{\partial\left(\frac{\beta F}{V}\right)}{\partial q} = 0 \qquad (7)$$

Simultaneous solution of the above set of equations gives the equilibrium Fourier coefficients f_{ij} and the smectic wavenumber q. The value of n is set such that the order of magnitude of $|f_{in}|$ cannot be larger than 10^{-4}. In our calculations, the maximum value of n never exceeded 12, even at very high pressures. It turned out that the first three order parameters can give an accurate representation of the positional distribution functions in all examined cases (see section 3).

In the following section we show equilibrium distribution functions along the smectic period for various smectic phases under different conditions. The distributions can be drawn from the equilibrium Fourier coefficients and smectic periods in each case. We pay special attention to the structure of the distribution profiles and their changes with varying length ratio ($l = L_2/L_1$) at a given pressure and composition. We make comparisons between the theoretical results and the corresponding experimental data whenever possible.

3. Results and Discussion

We use the mole fraction of long rods ($x = N_1/N$), the length ratio of the system ($l = L_2/L_1$), which is always less than one, and the pressure (P) as inputs of the theory and determine the mean density ($\rho = (N_1 + N_2)/V$), smectic period (d), and order parameters (f_{ij}) from minimization of the free energy. Available experimental data to compare with are the smectic period and the stability boundaries of the different smectic structures.

We start by presenting the four theoretically observed smectic structures. These were obtained at a given pressure and for different length ratios (see Figures 1−4). All results in these figures were obtained for a value of reduced pressure $P^* = \beta P v_1 = 4$, where v_1 is the particle volume of species 1. In the normal smectic A (S_1) phase, the short and long rods mix together completely, forming a layered structure made of identical layers (Figure 1). The distribution function of the long rods is more peaked than that of the short rods; i.e., the long rods are more localized at the center of the layer than the short rods. This is a consequence of the fact that the ends of the long particles are always closer to neighboring layers than the ends of the short rods sitting at the same average position. With such positional ordering, the packing of the rods is very efficient to reduce the excluded volume between particles of neighboring layers. The spectrum of smectic order parameters of the short rods shows that the first order parameter is the most dominant and that three order parameters are necessary to determine the correct distribution functions. This is also true for long rods, even if their order parameters (not shown in Figure 1) are slightly larger than those of short rods. Both the spectral shape and the magnitude of

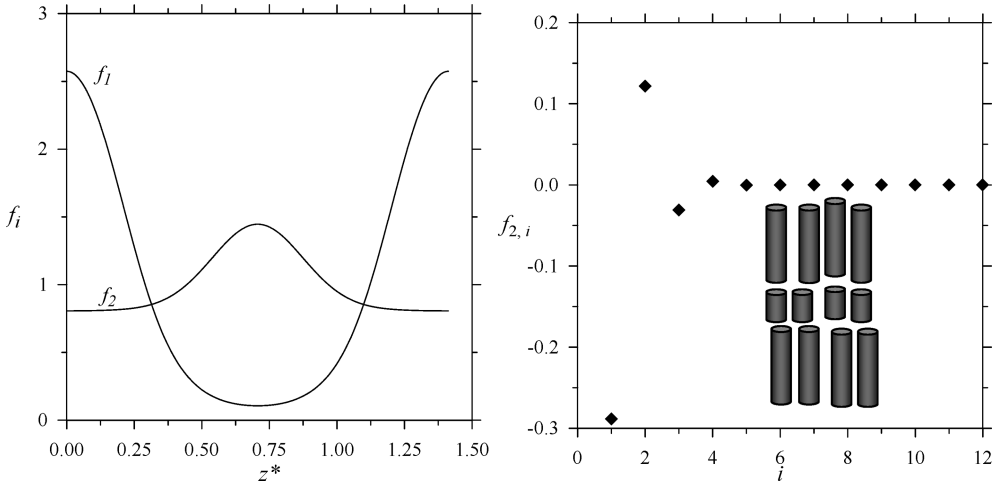

Figure 2. Microsegregated smectic phase (S_2) at $P^* = 4$ and for $l = 0.3$ and $x = 0.75$. Left panel: positional distribution functions of short and long rods as a function of $z^* = z/L_1$ in the interval $0 < z^* < d/L_1$. Right panel: Fourier spectrum of the short rods and the schematic of particle arrangement in S_2 structure.

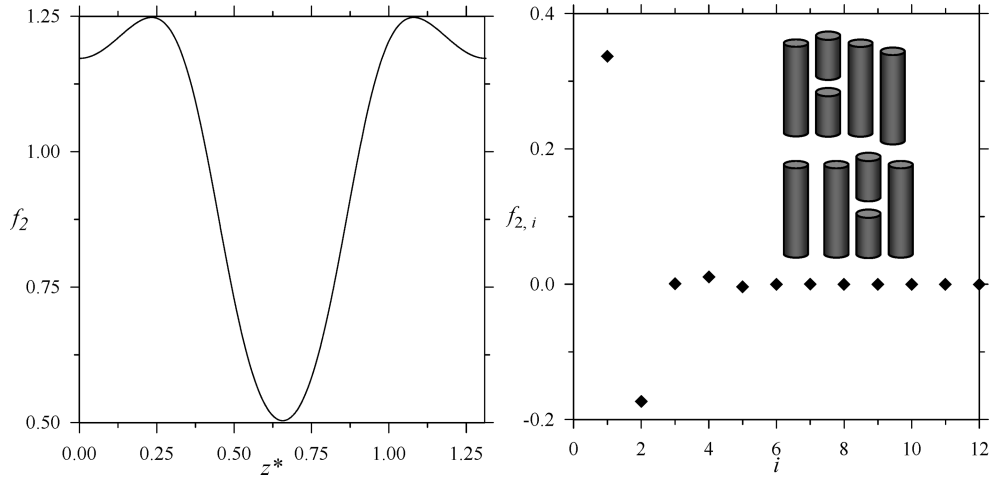

Figure 3. Two-in-one smectic phase (S_3) at $P^* = 4$ and for $l = 0.45$ and $x = 0.75$. Left panel: positional distribution function of short rods as a function of $z^* = z/L_1$ in the interval $0 < z^* < d/L_1$. Right panel: Fourier spectrum of the short rods and the schematic of particle arrangement in S_3 structure.

the order parameters of this smectic phase are consistent with X-ray results of Takanishi et al.[32] for smectic phases of one-component thermotropic liquid crystals. In the second smectic structure (S_2), the majority of the short rods have enough room to stay in the interstitial region, i.e., alternation of layers rich in short and long rods takes place, as shown by Figure 2 (note that a significant amount of short rods can still populate the long-rod layers). This corresponds to microsegregation of short and long rods. We must mention here that segregation of short and long rods can also occur in smectic phases rich in short rods. The reason why this structure can occur regardless of which rod type comes in greater number is the same: more efficient packing of rods can be achieved by minimizing the contact between overlapping layers and by more efficient filling of the interstitial region. The Fourier spectrum of the long rods looks like that of a normal smectic structure, while the first-order parameter of the short rods is negative due to the microsegregation. Therefore, we can say that the main feature of the S_2 structure is $f_{11} > 0$ and $f_{21} < 0$ ($f_{11} < 0$ and $f_{21} > 0$) when the long (short) rods are more abundant.

Okoshi et al.[26] have found that the spatial distribution of short rods is quite peculiar when the length of the long rod is approximately twice that of short rod ($l \approx 0.5$). In this new structure (S_3), the distribution of short rods exhibits *two* peaks inside one layer of the long rods. Therefore, S_3 can be referred to as *two-in-one* ordering. We can see from Figure 3 that Onsager theory indeed predicts the existence of two-in-one smectics. The intrinsic feature of the S_3 structure is a negative value of the second-order parameter of short rods. But in order for the distribution function to exhibit two peaks, a negative value of f_{22} is not enough: it has to exceed a threshold value. Later in this section we will give a more quantitative definition of two-in-one ordering.

Yet another new smectic structure emerges at length ratios intermediate between those characteristic of the S_2 and S_3 phases in long-rod-rich regions, as shown in Figure 4. The distribution of short rods is still double-peaked, but the position of the weaker peak corresponds to the center of the layer, while that of the stronger peak is in the interstitial region. This profile shows that the short particles tend to be in the interstitial region, but some of them still prefer to lie at the layers made of long rods. This new phase can be considered as a partially microsegregated smectic phase. Similarly to the problem of how to distinguish between the S_1 and S_3 phases, there is some trouble discriminating the spectra of the S_2 structure from that of the S_4 one, since they are very similar and differ only in magnitude. In order to determine the type of smectic structure, it is very important to analyze the positional distribution functions, which can be very hard for X-ray experiments since only the absolute value of the order parameters can be extracted.

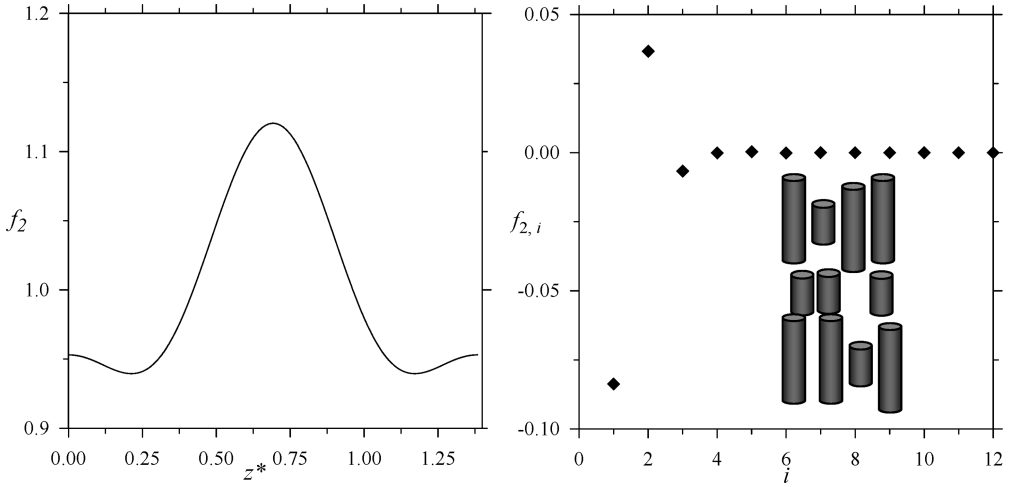

Figure 4. Partially microsegregated smectic phase (S_4) at $P^* = 4$ and for $l = 0.35$ and $x = 0.75$. Left panel: positional distribution function of short rods as a function of $z^* = z/L_1$ in the interval $0 < z^* < d/L_1$. Right panel: Fourier spectrum of the short rods and the schematic of particle arrangement in S_4 phase.

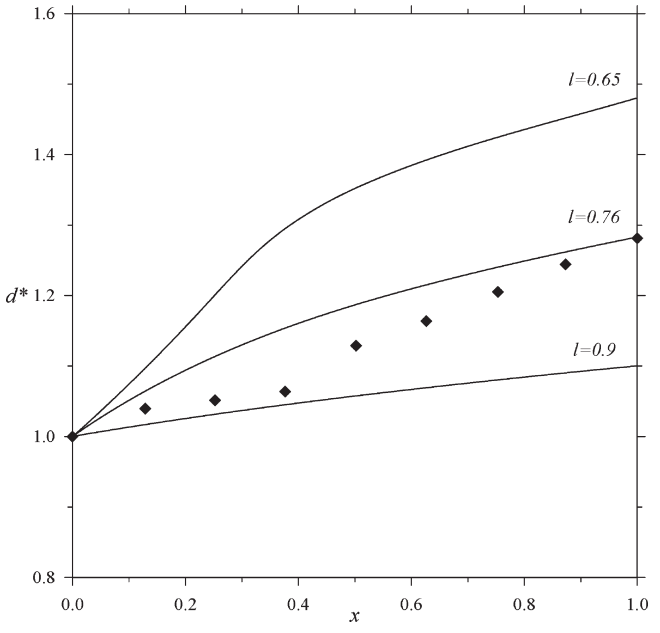

Figure 5. Smectic period of the S_1 structure vs composition for different length ratios ($l = L_2/L_1$) at $P^* = 5$. The experimental data (diamonds) of polysilanes,[26] as obtained from the q-vector location of the main peak in the X-ray diffraction pattern, correspond to $l = 0.76$, while the curves are the results from Onsager theory. The smectic period of the mixture is made dimensionless using the period of the one-component smectic phase made of short rods, i.e. $d^* = d/d(x = 0)$.

In addition, measurement of second- and third-order parameters is technically very difficult.

Now we are in a position to make some quantitative comparisons between the binary mixture of polysilanes and that of hard rods. The first example is the composition dependence of the smectic period of the S_1 phase, shown in Figure 5. The reduced pressure is set to a fixed value ($P^* = 5$) for all comparisons with the experiment in this paper. This choice for the pressure is dictated by our aim to reproduce the experimental results and the stability region of the smectic ordering accurately, since the smectic phase exists mainly in the interval $3 < P^* < 6$. In the figure the dimensionless period of the model mixture is compared to that of the real material. We choose to define a dimensionless period as ($d^* = d/d(x = 0)$), i.e., using the smectic period of the monodisperse short-rod limit, for both theory and experiment (the agreement for $x = 0$ is therefore perfect by definition). Our choice for the value of reduced pressure is fortunate because the agreement between theory and experiment is almost perfect in the other, $x = 1$, monodisperse limit for $l = 0.76$. Far from the monodisperse limits the agreement is not perfect, which may be attributed to the effect of dispersive attraction and/or defects of the theory. We also note from Figure 5 that the smectic period deviates from the experimentally observed linear behavior upon decreasing the length. The linear relation between d^* and x does not hold even for $l = 0.9$.

In the next two examples ($l = 0.47$ and 0.35) (see Figure 6), the phase rich in long rods forms a S_3 structure, while that rich in short rods is a S_2 structure, in both theory and experiment. To determine the theoretical stability boundary for S_3, we first calculate the distance (d_2) between the two peaks of the short-rod distribution function that lie inside the layer of long rods. The location of one of the peaks with respect to the layer center is obtained from the condition $f_2'(z) = 0$, and d_2 is given by twice this value. The composition range of the S_3 phase is now given by the nonzero values of d_2 in the interval $0 < d_2 < d$. In Figure 6 scaling of the period is made with the smectic period of the long rods; i.e., the theoretical and experimental results coincide at $x = 1$. In the figure the two sets of symbols, diamonds and circles, correspond to the smectic period as obtained from (independent) measurements of the q-vector location of the first-order (diamonds) and second-order (circles) reflections in the experimental X-ray diffraction patterns; whenever the two branches coexist, their values should be related by a factor of 2, the larger one giving the true smectic period. In correspondence, the two theoretical branches (continuous curve, which is the true smectic period, and the dashed curve) are related by a factor of 2. We can say that the agreement between theory and experiment is satisfactory, because the theoretical and experimental periods are close to each other, as well as the mole fraction range where the S_3 structure is predicted to be stable by the theory. Both experiment and theory show that a decreasing length ratio shrinks the stability region of S_3 phase. We again suspect that the effect of attractive forces acting between polysilane molecules is not negligible at the experimental (ambient) temperature, because the smectic ordering is stable at any composition in the real sample, whereas in the model there are regions in composition where the stable phase is nematic. In the case of our model hard rods, the smectic phase is replaced by the nematic one for intermediate compositions. For $l = 0.35$ the smectic phase does not even exist in the one-component phase of short rods. Indeed,

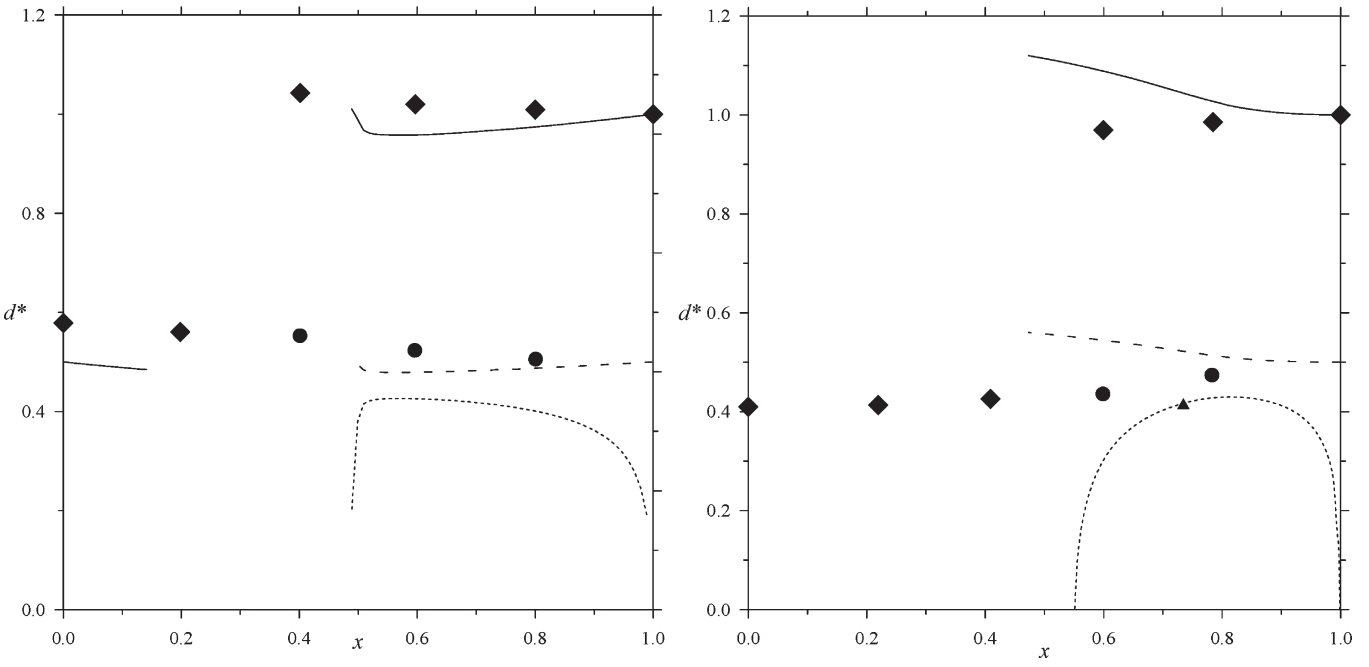

Figure 6. Smectic period vs composition for (left panel) $l = 0.47$ and (right panel) $l = 0.35$ at $P^* = 5$. Continuous curve shows the theoretical smectic period (dashed curve is half the theoretical smectic period in the S_3 structure), while the short-dashed curve is the theoretical result for the distance between the neighboring short-rod layers inside a smectic layer, d_2, in the S_3 structure. Diamonds represent the experimental smectic periods as obtained from first-order X-ray reflections,[26] with circles being obtained from second-order reflections whenever two reflections are present (see text). The smectic period of the mixture is made dimensionless using the period of the one-component smectic phase made of long rods, i.e., $d^* = d/d(x = 1)$. In right panel the triangle denotes the boundary between S_3 and S_4 structures. For lower (higher) mole fractions, S_4 (S_3) is the stable structure.

strong side-by-side attractive interactions between long rods definitely promote layer formation. The distance between the peaks of short rods (d_2) is also shown in Figure 6. We can see that d_2 vanishes as the nematic region or the one-component system of long rods is approached. Note that this quantity is always less than half a period and is not measurable experimentally.

In Figure 7 the length ratio dependence of the smectic period is presented at the same pressure ($P^* = 5$) and for composition ($x = 0.75$). Data from the polysilane mixture at the experimental conditions[26] are indicated using symbols, as in Figure 6. For large l the stable smectic structure is the normal one (S_1) down to $l \approx 0.58$, according to both theory and experiment. For lower values of length ratio, the stable phase changes to S_3. The S_1-S_3 stability boundary coincides almost perfectly with the experimental data. The stable smectic structure is of type S_3 all the way down to the lowest value of length ratios analyzed. The theoretical smectic period agrees very well with experiment in the whole range of composition, in particular, in the S_3 region. Note that, again, the dashed curve is exactly half the theoretical smectic period. However, we can also see that the destabilization of smectic ordering takes place in the model for $l < 0.4$, while the smectic phase is stable at lower length ratios in the polysilane mixture. In Figure 7 we have also plotted the d_2 distance, which obviously tends to zero as the smectic structure changes from S_3 to S_1.

In the light of the above results, we can conclude that the hard-cylinder model is a good representation of polysilanes but does not capture all the fine details of the interaction. This can be attributed to the dispersion interactions acting between the polymers. We do not think that length polydispersity in the two components should be an essential ingredient of the model because polydispersity always works against smectic ordering and tends to destabilize layering, which is not the case here.

Finally, we make some predictions for the stability of the peculiar two-in-one (partially microsegregated) ordering in the length ratio−composition plane and for different values of the pressure.

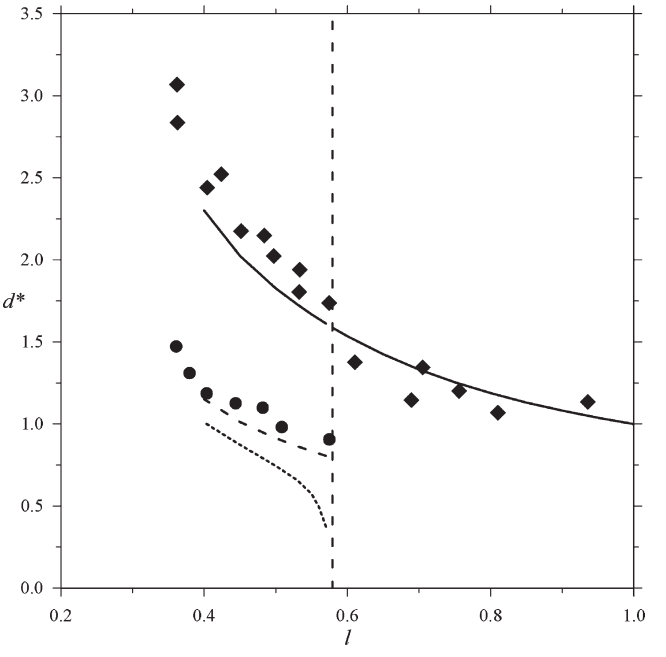

Figure 7. Smectic period vs length ratio at $P^* = 5$ and for $x = 0.75$. Continuous curves show the theoretical smectic period; dashed curve is half the smectic period in the S_3 structure. Diamonds are the experimental results for the smectic period,[26] as obtained from the first-order reflections in the X-ray diffraction patterns; circles are obtained from the second-order reflections, which are present in the experimentally measured S_3 structure. The vertical dashed line delimits the regions where S_1 (right) and S_3 (left) structures are stable, while the short-dashed curve shows the theoretically obtained distance between the neighboring short-rod peaks inside a smectic layer, d_2. The smectic period of the mixture is made dimensionless using the period of the one-component smectic made of long rods, i.e., $d^* = d/d(x = 1)$.

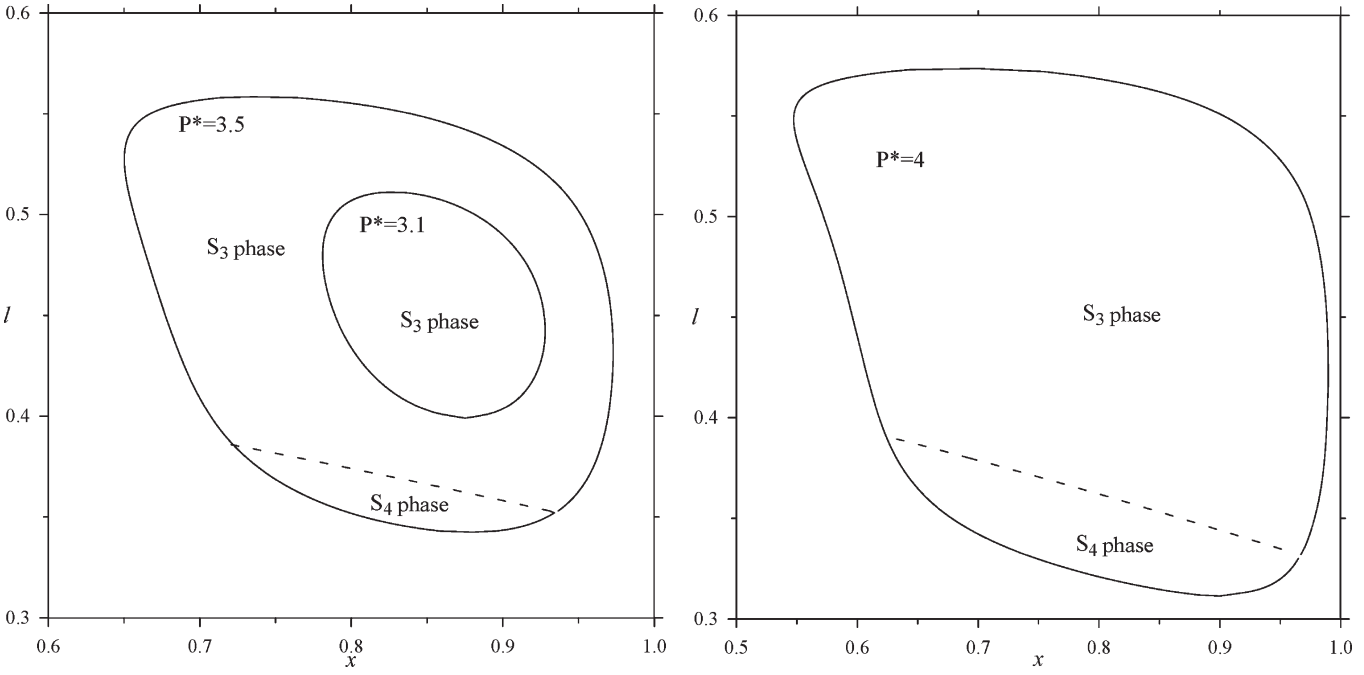

Figure 8. Closed-loop stability regions of S_3 and S_4 structures in length ratio−composition plane for (left panel) $P^* = 3.1$ and 3.5 and (right panel) $P^* = 4$. Inside the loop the S_3 and S_4 structures are stable, while S_1 and S_2 structures form outside the loop. The dashed curve shows the boundary between the S_3 and S_4 structures. The curves are the results from Onsager theory.

Table 1. Length Ratio Dependence of the Regions Where the Different Smectic Phases Are Stable for the Experimental Polysilane Binary Mixture and for the Model Hard-Cylinder Mixture According to the Theory

smectic structure	experiment	theory
S_1	$0.59 < l < 1$	$0.58 < l < 1$
S_2 (long rod rich phase)	−	$l < 0.39$
S_2 (short rod rich phase)	$0.36 < l < 0.59$	$0.32 < l < 0.56$
S_3	$0.36 < l < 0.59$	$0.33 < l < 0.58$
S_4	−	$0.3 < l < 0.39$

Figure 8 shows the island where the S_3 and S_4 structures are stabilized. At low pressures, only the S_3 structure is stable in a narrow range of length ratios and compositions, while the S_4 structure does not exist. With increasing pressure, the island of S_3 widens in all directions, and the S_4 phase forms at low length ratios. The possibility of experimental detection of S_4 ordering increases with increasing pressure (density). The reason why the island becomes wider is that the increasing pressure is accompanied by a higher density, which forces the system to adopt a more efficient packing. The more efficient packing corresponds to arrangements into S_3 and S_4 structures in a mixture of hard cylinders. The existence of upper and lower length ratio boundaries for S_3 can be explained as follows. In smectic phases rich in long rods, the smectic period is roughly speaking about $1.3L_1$. This means that there is still enough room for two layers of short rods to accommodate, provided they are shorter than about $0.6L_1$, without the risk of overlapping with the neighboring layers. The geometrical restriction behind the occurrence of a lower bound is that short rods with lengths less than about $0.3L_1$ can enter the interstitial region and form a layer which makes the system more efficiently packed than in the two-in-one structure. The results of our study for the stability regions of the different smectic structures are collected in Table 1, together with the available experimental data. We can see that the stability ranges in length ratios for the different smectic structures of polysilanes are accurately reproduced by the hard-cylinder model. Our model needs refinements only for the accurate determination of the smectic periods.

4. Conclusions

We have shown that binary mixtures of polysilanes can be modeled as a mixture of short and long hard cylinders in the smectic phase. Our study is a clear example where a hard-body model is capable of reproducing all smectic structures of an experimental system without the inclusion of effects arising from polydispersity, flexibility, polarity, and soft interactions. It is also true that the polysilane polymer is a very ideal particle because it is nonpolar, rigid, and rodlike. Other experimental colloidal systems such as mineral-based liquid crystals and the solution of viruses, which are widely considered as a playground for hard-body models, can be also represented by suitably chosen hard-body models in which several effects (flexibility, chirality, polydispersity, and Coulombic interactions) are taken into account. However, because of the mapping problems between the colloidal dispersions and hard-body systems, the system of polysilane polymers seems to be more suitable for future tests of Onsager theory and simulation studies.

The present study also reveals the weaknesses of the hard-cylinder model. It is not capable, by construction, of accounting for the thermotropic character of the polysilanes even in the smectic phase: while the hard-body model predicts strong destabilization of the smectic phase with respect to the nematic one, a binary mixture of polysilanes shows smectic ordering in the entire range of the composition. To reproduce this feature of the experimental system would require the use of higher pressures in the theory, a range that would belong to the more ordered columnar phase. To capture the above features of the polymer mixture, such dispersion interactions should be included in the hard-cylinder model, which favor the side-by-side configuration molecules. In this way the smectic phase can be stabilized at lower pressures. Addition of such interactions to the model would not affect substantially the relative stability of the different smectic structures because of the dominance of packing constraints.

Finally, we make some remarks about the approximations used in the theory. The assumption of perfect orientational order, and the use of a second-virial theory such as Onsager's, are very profitable with a view to simplifying the numerical calculations.

The first approximation is reasonable even though the occurrence of stable columnar phase in the system of bidisperse freely rotating hard rods is unlikely, while the second one is certainly questionable in very dense smectic phases. Onsager theory makes acceptable predictions for the critical density of the nematic−smectic phase transition, but the pressure is poorly reproduced both in nematic and smectic phases, mainly due to its neglect of higher-order density correlations. For example our choice for the pressure ($P^* = 5$) does not correspond to the experimental pressure value. An additional problem is that the smectic period is always overestimated. To solve the problem of the smectic period, the orientational entropy and a better treatment of correlations have to be included into the theory. The use of more advanced theories, such as the (still not fully developed) extension to free rotations of fundamental-measure theory for parallel cylinders,[35−37] would be beneficial to obtain better quantitative agreement between theory and experiment. It would be also important to perform new MC simulation studies to give further justifications for the existence of S_3 and S_4 phases in the mixture of short and long hard rods.

Acknowledgment. Support from grants S-0505/ESP-0299 from the Comunidad Autónoma de Madrid, FIS2007-65869-C03-01 and FIS2008-05865-C02-02 from the Ministerio de Educación y Ciencia of Spain, and the Hungarian-Spanish Integrated-Actions grant (HH2006-0005) is acknowledged.

References and Notes

(1) Barrat, J.-L.; Hansen, J.-P. *Basic Concepts for Simple and Complex Liquids*; Cambridge University Press: Cambridge, 2003.
(2) Hoshino, M.; Nakano, H.; Kimura, H. *J. Phys. Soc. Jpn.* **1979**, *46*, 1709.
(3) Frenkel, D.; Lekkerkerker, H. N. W.; Stroobants, A. *Nature* **1988**, *332*, 822.
(4) Veerman, J. A. C.; Frenkel, D. *Phys. Rev. A* **1992**, *45*, 5632.
(5) Onsager, L. *Ann. N.Y. Acad. Sci.* **1949**, *51*, 627.
(6) Vroege, G. J.; Lekkerkerker, H. N. W. *Rep. Prog. Phys.* **1992**, *55*, 1241.
(7) Davidson, P.; Gabriel, J. C. P. *Curr. Opin. Colloid Interface Sci.* **2005**, *9*, 377.
(8) Strey, H. H.; Parsegian, V. A.; Podgornik, R. *Phys. Rev. Lett.* **1997**, *78*, 895.
(9) Dogic, Z.; Fraden, S. *Curr. Opin. Colloid Interface Sci.* **2006**, *11*, 47.
(10) Buitenhuis, J.; Donselaar, L. N.; Buining, P. A.; Stroobants, A.; Lekkerkerker, H. N. W. *J. Colloid Interface Sci.* **1995**, *175*, 46.
(11) Sluckin, T. J. *Liq. Cryst.* **1989**, *6*, 111.
(12) Bates, M. A.; Frenkel, D. *J. Chem. Phys.* **1998**, *109*, 6193.
(13) (a) Okoshi, K.; Kamee, H.; Suzaki, G.; Tokita, M.; Fujiki, M.; Watanabe, J. *Macromolecules* **2002**, *35*, 4556. (b) Oka, H.; Suzaki, G.; Edo, S.; Suzuki, A.; Tokita, M.; Watanabe, J. *Macromolecules* **2008**, *41*, 7783.
(14) van der Kooij, F. M.; Lekkerkerker, H. N. W. *Phys. Rev. Lett.* **2000**, *84*, 781.
(15) Purdy, K. R.; Varga, S.; Galindo, A.; Jackson, G.; Fraden, S. *Phys. Rev. Lett.* **2005**, *94*, 057801.
(16) Koda, T.; Kimura, H. *J. Phys. Soc. Jpn.* **1994**, *63*, 984.
(17) Cinacchi, G.; Mederos, L.; Velasco, E. *J. Chem. Phys.* **2004**, *121*, 3854.
(18) Varga, S.; Velasco, E.; Mederos, L.; Vesely, F. J. *Mol. Phys.* **2009**, *107*, 2481.
(19) Stroobants, A. *Phys. Rev. Lett.* **1992**, *69*, 2388.
(20) Cinacchi, G.; Velasco, E.; Mederos, L. *J. Phys.: Condens. Matter* **2004**, *16*, S2003.
(21) Martínez-Ratón, Y.; Velasco, E.; Mederos, L. *J. Chem. Phys.* **2005**, *123*, 104906.
(22) Cui, S. M.; Chen, Z. Y. *Phys. Rev. E* **1994**, *50*, 3747.
(23) van Roij, R.; Mulder, B. *Phys. Rev. E* **1996**, *54*, 6430.
(24) Varga, S.; Purdy, K. R.; Galindo, A.; Fraden, S.; Jackson, G. *Phys. Rev. E* **2005**, *72*, 051704.
(25) Cinacchi, G.; Martínez-Ratón, Y.; Mederos, L.; Velasco, E. *J. Chem. Phys.* **2006**, *124*, 234904.
(26) Okoshi, K.; Suzuki, A.; Tokita, M.; Fujiki, M.; Watanabe, J. *Macromolecules* **2009**, *42*, 3443.
(27) Mulder, B. *Phys. Rev. A* **1987**, *35*, 3095.
(28) Sear, R. P.; Jackson, G. *Phys. Rev. E* **1995**, *52*, 3881.
(29) Sear, R. P.; Jackson, G. *Mol. Phys.* **1994**, *83*, 961.
(30) Sear, R. P.; Jackson, G. *J. Chem. Phys.* **1995**, *102*, 2622.
(31) Leadbetter, A. J.; Norris, E. K. *Mol. Phys.* **1979**, *38*, 669.
(32) Takanishi, Y.; Ikeda, A.; Takezoe, H.; Fukuda, A. *Phys. Rev. E.* **1995**, *51*, 400.
(33) Okoshi, K.; Saxena, A.; Fujiki, M.; Suzaki, G.; Watanabe, J.; Tokita, M. *Mol. Cryst. Liq. Cryst.* **2004**, *419*, 57.
(34) Kapernaum, N.; Giesselmann, F. *Phys. Rev. E* **2008**, *78*, 062701.
(35) Martínez-Ratón, Y.; Capitán, J. A.; Cuesta, J. A. *Phys. Rev. E* **2008**, *77*, 051205.
(36) Cinacchi, G.; Schmid, F. *J. Phys.: Condens. Matter* **2002**, *14*, 12223.
(37) Hansen-Goos; Mecke, H. K. *Phys. Rev. Lett.* **2009**, *102*, 018302.